Accurate calculation of near-critical heat capacities C_P and C_V of argon using molecular dynamics

Jakler Nichele [a,b], Alan B. de Oliveira [c], Leonardo S. de B. Alves [d], Itamar Borges, Jr [a,b,*]

[a] Defense Engineering Graduate Program, Military Institute of Engineering, Rio de Janeiro, RJ 22290-270, Brazil
[b] Chemical Engineering Department, Military Institute of Engineering, Rio de Janeiro, RJ 22290-270, Brazil
[c] Department of Physics, Federal University of Ouro Preto, Ouro Preto, MG 35400-000, Brazil
[d] Theoretical and Applied Mechanics Laboratory, Mechanical Engineering Department, Fluminense Federal University, Niteroi, RJ 24210-240, Brazil

ARTICLE INFO

ABSTRACT

Molecular dynamics (MD) employing the Lennard-Jones (LJ) interaction potential was used to compute the heat capacities of argon at constant volume C_V and constant pressure C_P near the critical point very close to the asymptotic region. The accurate MD calculation of critical divergences was shown to be related to a careful choice of the cutoff radius r_c and the inclusion of long-range corrections in the LJ potential. The computed C_P and C_V values have very good agreement as compared to available NIST data. Furthermore, values of C_V in a range of temperatures for which NIST data is not available could be computed. In the investigated range of temperatures, both C_P and C_V MD results were fitted to a simple mathematical expression based on an empirical model that describes the critical effects when the asymptotic models are not appropriate. The present approach is of general applicability and robust to compute thermophysical properties of fluids in the near-critical region.

© 2017 Elsevier B.V. All rights reserved.

1. Introduction

The investigation of critical phenomena in real fluids is not simple. It is well known when tracking properties of fluids approaching the critical point that an anomalous behavior can be observed. Depending on the investigated property, this is generally characterized by a strong divergence to infinity or a fast collapse to zero [1,2]. Such an anomalous behavior, which is due to the increasing spatial correlation of fluid molecules, appears in the form of large-scale density fluctuations close to the criticality [3].

Experiments with near-critical fluids are complex to perform because they require high precision apparatuses and very specific experimental methods to capture critical divergences [2,4]. Furthermore, near-critical fluids take longer times to equilibrate [5] and are highly sensitive to gravitational fields due to the strong compressibility [1,6] and to the presence of even small amounts of impurities [7–10]. Depending on the extension of the investigation, there are severe experimental limitations as explicitly displayed in the NIST database by the limited range of available values of fluid properties near to the critical point [11].

On the theoretical side, a considerable effort has been made to describe critical phenomena. Mean field approaches, the workhorse of

classical statistical mechanics, are not suitable to describe critical divergences because long range correlations are not included by construction [5]. The use of power laws based on the concept of universal scaling was an important step to overcome that difficult [12]. Undoubtedly, the most significant contribution to this field is the development of the renormalization group (RG) theory that established a new general framework to elucidate the critical behavior [13]. From this theoretical framework, it was possible to identify classes of systems that behave similarly near to the critical point. Therefore, even systems with completely different physical nature but belonging to the same universality class have their critical divergences described by the same universal exponents depending only on the property under consideration. For instance, simple fluids near the critical point belong to the same class of 3D Ising-like systems due to the short-range forces and the presence of only one order parameter [14].

In spite of the great success of RG theory to describe the anomalous behavior of fluid properties near the critical point, only in the asymptotic limit close to the critical point this theory leads to quantitative agreement between theory and experiment. In order to experimentally capture asymptotic divergences, it is necessary, for instance, to measure temperatures of the order of 10^{-3} K or less, which is not simple. Moreover, away from the critical point asymptotic power laws are not adequate to model fluid properties [15]. In this case, it would be necessary to extend the RG predictions to a larger range of thermodynamic states beyond the vicinity of the critical point in the phase diagram [16–18]. Possible approaches include crossover models, which focus on the

development of theoretical models capable of describing continuously fluids from 3D Ising to mean-field-like behaviors [19–21]. Molecular simulations can be especially helpful to compute values of physical properties in the near-critical region. Molecular dynamics (MD) and Monte Carlo methods are well-established molecular simulation techniques that can be used to investigate critical phenomena. Recently, we employed MD to compute accurate values of isothermal compressibility and thermal expansion coefficient [22] as well as transport properties [23] of argon near the critical point.

In this work, two thermodynamic properties with great practical interest are investigated: the heat capacities at constant volume, C_V, and at constant pressure, C_P. Their importance stems from application to engineering problems related to the analysis of energy balance in industrial processes, heat transfer and fluid dynamics. The former property is actually the most difficult one we have calculated so far [22,23], which is an important fact that delayed and motivated the present work. This is the major reason why the definition of a calculation protocol is deemed useful and presented here. It starts by noting that C_V and C_P are basic thermodynamic properties defined as temperature (T) derivatives of the internal energy (E) and the enthalpy (H), respectively, along specific paths in the phase diagram: [24]

$$C_V = \left(\frac{\partial E}{\partial T}\right)_V \tag{1}$$

$$C_P = \left(\frac{\partial H}{\partial T}\right)_P \tag{2}$$

Many recent works investigate the heat capacities of fluid systems near the critical point [4,20,25–39]. Both theory and experiment indicate that isochoric and isobaric heat capacities – C_V and C_P – of near-critical fluids have an anomalous divergent behavior in this thermodynamic region [40–42]. The asymptotic divergent behavior of C_V along the critical isochoric can be described as a power law of the temperature T in the form

$$C_V = C_{Vo}(\Delta T_r)^{-\alpha} \tag{3}$$

where $\Delta T_r = T/T_c - 1$, T_c is the critical temperature, C_{Vo} is a cofactor that depends on the substance and α is a universal exponent [19]. In contrast, the critical divergence of C_P can be deduced employing the generalized Mayer's relation [24] given by

$$C_P - C_V = \frac{TM}{\rho^2}\left(\frac{\partial \rho}{\partial T}\right)_P^2\left(\frac{\partial P}{\partial \rho}\right)_T \tag{4}$$

for which P is the pressure, ρ is the density and M is the molar mass and which can be used to show that the asymptotic behavior of C_P and of the isothermal compressibility $K_T = (1/\rho)(\partial \rho/\partial P)_T$ is similar, [1] i.e.

$$C_P \approx C_{Po}(\Delta T_r)^{-\gamma} \tag{5}$$

since $K_T = K_{To}(\Delta T_r)^{-\gamma}$. The α and γ exponents of Eqs. (3) and (5) were accurately determined from experiments and RG calculations, yielding $\alpha = 0.110 \pm 0.003$ and $\gamma = 1.239 \pm 0.002$ [43].

The correlation length ξ, which measures the spatial extension of correlated structural fluctuations, also diverges asymptotically as a function of temperature according to a power law given by [3,14]

$$\xi = \xi_o(\Delta T_r)^{-\nu} \tag{6}$$

in such a way that it becomes much larger than any microscopic length of the system. In this regime it is reasonable to assume ξ as the only relevant length of the fluid [33]. In Eq. (6), $\nu = 0.630 \pm 0.001$ is a universal critical exponent [43] and the cofactor ξ_o for argon is 1.4 Å [44]. Therefore, in the vicinity of the critical point, the role of long-range

interactions increases and fluid properties cannot be sufficiently described by a local microscopic behavior – it is then essential to take into account the collective motion of the fluid particles.

The computation of C_V near the critical point is especially more challenging compared to C_P because changes in internal energy (E) for a given change in temperature are much smaller than the respective enthalpy (H) changes. In other words, C_V diverges weakly while C_P diverges strongly [14]. Moreover, in the neighborhood of the critical point, the calculation of C_V with Eq. (1) can be difficult due to the magnitude of the microscopic fluctuations of E.

A fluid composed by argon atoms has great importance for theoretical and practical reasons. Argon is the most abundant noble gas in Earth's atmosphere and is chemically inert for practical purposes, which makes it very useful to calibrate experimental devices, for example. As a noble gas, argon atoms are nonpolar, nonbonded and their interactions are well described by the classical Lennard-Jones (LJ) interaction potential. This potential is the simplest model that incorporates both the overlap of the electronic molecular clouds (responsible for the repulsion between atoms) and the van der Waals interaction that accounts for the weak attraction between particles. Not surprisingly, due to its simplicity the LJ potential is frequently used in molecular simulations. Furthermore, theoretical studies with argon are especially important because they can be a starting point for further investigations related to other spherically symmetric species. One can also find a large body of high quality experimental data related to argon properties [11] – including C_V and C_P values [41], which makes the comparison with computational results more interesting. It is not a coincidence that argon has been extensively used in molecular dynamics simulations since the first studies [45].

In this work we use MD as a robust general approach to compute accurate results of C_P and C_V of argon in the neighborhood of the critical point. The computed results compare very favorably with available NIST data [11]. In addition to present accurate results for these properties under conditions experimentally difficult to attain, we computed C_V values in a thermodynamic region where NIST data is limited and theoretical values are poor. Finally, we discuss how numerical parameters in MD simulations affect the accuracy of the results for near-critical fluids.

2. Computational details

Molecular dynamics techniques compute phase space trajectories – positions r_i and velocities v_i – of a system of particles through numerical simulations driven by Newton's equations of motion [46–48]. From the phase space, thermodynamic properties can be computed based on ensemble averages as deduced in statistical mechanics. A general view of the procedures for employing molecular dynamics to study near-critical fluids is presented in details in Ref. [49].

The accuracy of MD results strongly depends on the adequate selection of numerical parameters. We used 10^4 argon atoms to achieve a precise control of the thermodynamic state within the cubic simulation box. Periodic boundary conditions were employed to avoid edge effects on the bulk fluid. The time step was 1 fs. Each state was equilibrated during 2 ns and additional 2 ns were used to compute the averages. Energies and enthalpies were computed at twenty unequally spaced values of ΔT_r between 0.00 and 1.00 clustered near the critical point. The values of ΔT_r are listed in the supplementary material. C_V and C_P were computed using Eqs. (1) and (2) at the midpoint of each ΔT_r interval resulting in nineteen values.

Simulations were performed with LAMMPS package [50]. For the interatomic potential, we used the truncated version of the Lennard-Jones interaction, written as

$$U(r_{ij}) = \begin{cases} 4\varepsilon\left[(\sigma/r_{ij})^{12} - (\sigma/r_{ij})^6\right] + U_{TC} & (r_{ij} \leq r_c) \\ 0 & (r_{ij} > r_c) \end{cases} \tag{7}$$

where U_{TC} is the so-called tail correction given by [48,51]

$$U_{TC} = 2\pi n \int_{r_c}^{\infty} r_{ij}^2 g(r_{ij}) U(r_{ij}) dr_{ij} \qquad (8)$$

where n is the number density N/V, $g(r_{ij})$ is the pair distribution function, ε is the energy well depth, σ is the effective atom size, r_{ij} is the distance between particles i and j, and r_c is the cutoff radius. The 12-exponent term describes the repulsion at short distances whereas the 6-exponent term stands for the attraction at larger separations [52, 53]. Here we used $\varepsilon/k_B = 119.8$ K and $\sigma = 3.405$ Å [54]. The critical constants of the same Lennard-Jones system were computed previously [55–57] resulting in $T_c = 157.178$ K, $P_c = 52.8862$ atm, and $\rho_c = 530.892$ kg/m³. The NIST tables, however, report $T_{c\text{-NIST}} = 150.687$ K, $P_{c\text{-NIST}} = 47.9441$ atm and $\rho_{c\text{-NIST}} = 535.599$ kg/m³ [11]. This discrepancy was overcome by using reduced variables which provides a suitable way to compare NIST heat capacities with the corresponding present MD results. The used ε and σ values were also employed in the computation of more complex properties such as the bulk viscosity [23,58].

The calculation of C_V performed within the *NVT* ensemble employed two density values: $\rho = \rho_c$ and $\rho = 1.2\rho_c$. For C_P, the *NPT* ensemble was used along with two pressure values, $P = P_c$ and $P = 1.2P_c$. The choice of 20% larger values of ρ_c and P_c are based on previous works [22,23]; however, other density and pressure values can be used. *NPT* and *NVT* ensembles were achieved by means of Nosé-Hoover barostat and thermostat [59].

Smaller cutoff radii in Eq. (7) are useful to reduce the computational cost of simulations by avoiding calculations over distant particles which would yield negligible interaction energies. Typical choices for r_c lie around 2.5σ, value indicated on classical textbooks, which neglect U_{ij} interaction values between one and 2% of ε [46]. However, considerably larger values for r_c are required to properly deal with near-critical fluids with correspondingly increase of computational cost [20,31,32,60]. For example, values for r_c up to 15σ have been used in studies that demand high quality radial distribution functions [61]. The sensitivity of our calculations with respect to this parameter was investigated for $r_c = 2.5\sigma$, 5.0σ, 7.5σ and 10.0σ. Such a large range of values for r_c was chosen based on the fact that some properties of near-critical fluids are especially affected by cutoff values below 5.0σ [60,62,63], in special the critical point value.

It is also important to note that MD simulations with periodic boundary conditions must obey the minimal image convention, which establishes that the length of the simulation box (L_{box}) must be greater than $2r_c$ to avoid multiple evaluations of the interaction energy of the same pair of atoms. Moreover, the accurate description of the critical behavior requires at each temperature a simulation box larger than the correlation length. The number of particles in this work was chosen in order to keep the length of simulation box L_{box} larger than both $2r_c$ and the correlation length ξ, as shown in Fig. 1. The correlation length was estimated from Eq. (6). It can be seen that the only value of ΔT_r which leads to a $L_{box} < \xi$ is $\Delta T_r = 0$.

3. Results and discussion

Results for C_V as a function of ΔT_r at $\rho = \rho_c$ are presented in Fig. 2. This figure shows the results for $r_c = 7.5\sigma$, value that lead to the best compromise between agreement with NIST data and computational cost. At $\rho = \rho_c$, the $r_c = 2.5\sigma$ value poorly described the near-critical divergences. Improved results were obtained for $r_c = 5.0\sigma$, but considerably dispersion was still observed in the results. On the other hand, the use of $r_c = 10.0\sigma$ increased the computational time with negligible improvement of accuracy as compared to 7.5σ. Considering that tail corrections only change the total energy E by a constant value, C_V is not affected because it is computed from a derivative. Our data for C_V
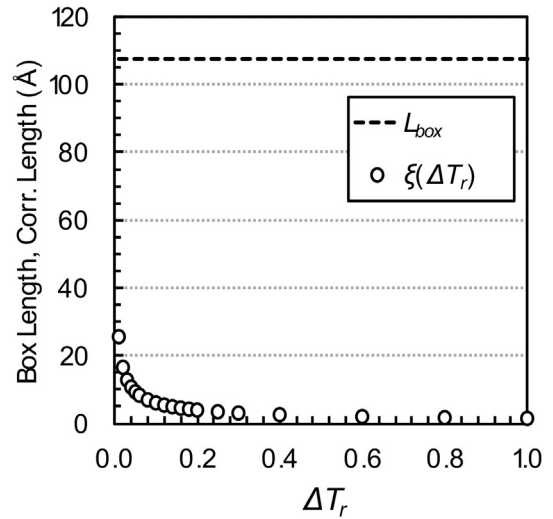

Fig. 1. Comparison between the box size and the corresponding correlation length ξ for C_V calculations at $\rho = \rho_c$ estimated from Eq. (6) for each considered ΔT_r value.

using $r_c = 2.5\sigma$, 5.0σ, and 10.0σ are presented in Fig. S1 of Supplementary material.

From the computed results, we propose an empirical model based on Refs. [20,64] that suitably fits the simulations results in the studied range of temperatures thereby capturing the critical effects when the asymptotic model is not appropriate. This model is described by the expression.

$$C_V = a(\Delta T_r)^{-b} + C_{V(i.g.)} \qquad (9)$$

where a and b are non-universal parameters, and $C_{V(i.g.)} = 3R/2 = 2.981$ cal/mol is the heat capacity of an ideal gas, with R being the ideal gas constant. The model of Eq. (9) is plotted in Fig. 2 as a dashed line with parameters a and b obtained in the fitting given in Table 1. Note that in this model the limiting behavior for gases at high temperatures must approach the ideal gas value. Fig. 2 shows the good agreement between MD results and NIST data as well as the robustness of
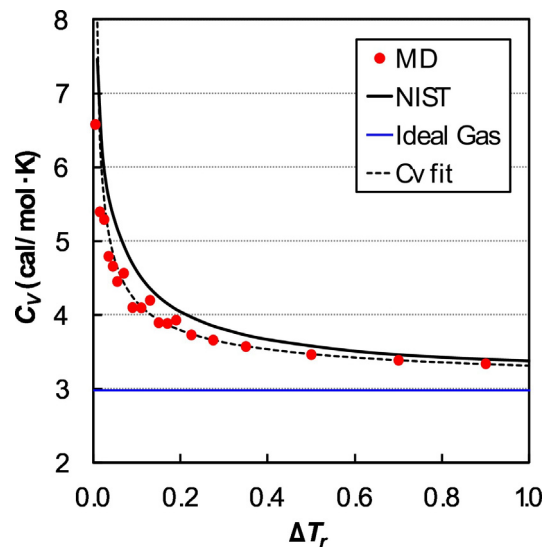

Fig. 2. Heat capacity at constant volume C_V obtained from MD simulations of 10^4 argon atoms as a function of temperature at $\rho = \rho_c$ using the Lennard-Jones potential with $r_c = 7.5\sigma$ and long range tail corrections. Full line: NIST values. Blue line: ideal gas value. Dashed line: fitted function to MD results according to Eq. (9). (For interpretation of the references to colour in this figure legend, the reader is referred to the web version of this article.)

Table 1
Fitting parameters for C_V and C_P using respectively Eqs. (9) and (10) from MD results and NIST data.

	Parameters	MD	NIST
C_V at	a (cal/mol)	0.3323	0.3898
$\rho = \rho_c$	b	0.5551	0.6136
C_P at	c (cal/mol)	1.0608	0.99971
$P = P_c$	d	0.80102	0.83876

Eq. (9) to fit our MD results for a wide range of temperatures, including points very close to the critical temperature, i.e., $\Delta T_r = 0.05$. The plot of the fitting curve reveals that the fitting has an average error of 8% as compared to NIST data especially in the interval $0.04 \leq \Delta T_r \leq 0.50$.

To assure the accuracy of the previous results, Fig. 3 demonstrates how the average pressures computed with NVT simulations can suitable describes the corresponding experimental values. The overall average error along the curve is <4%. Below $\Delta T_r = 0.30$ the error for the computed pressure is <2%.

Fig. 4 presents values for C_P at $P = P_c$ for $r_c = 7.5\sigma$. As expected, C_P is affected by the r_c values and the inclusion or not of long-range corrections. For example, the choice $r_c = 2.5\sigma$ is enough to lead to a good agreement with NIST data but only by including the long-range corrections. On the other hand, simulations without long-range corrections give good results solely for $r_c \geq 7.5\sigma$. Results are not improved for $r_c = 10.0\sigma$ if compared to the ones obtained with 7.5σ. Additional results of C_P for $r_c = 2.5\sigma$, 5.0σ and 10.0σ with long range corrections are presented in the Fig. S2 of the Supplementary material.

In the same way as done for C_V, Fig. 5 presents how the average reduced densities ρ_r computed with NPT simulations can suitably describe the corresponding experimental values. Only at $\Delta T_r = 0.00$ the MD density values were overestimated by 25%. For the other ΔT_r values, the average error is 5%.

Similarly to the C_V results, we fitted the C_P MD values to an empirical power law given by

$$C_P = c(\Delta T_r)^{-d} + C_{P(i.g.)} \tag{10}$$

where c and d are non-universal parameters (given in Table 1), and $C_{P(i.g.)}$ is the heat capacity at constant pressure of an ideal gas equals $5R/2 = 4.968$ cal/mol; R is the ideal gas constant. The fitted function, Eq. (10), is plotted as a dashed line in the Fig. 4. The convergence of C_P
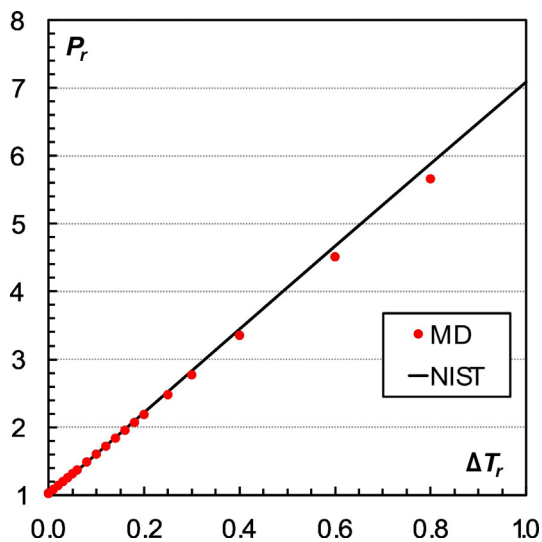

Fig. 4. Heat capacity at constant pressure C_P obtained from MD simulations of 10^4 argon atoms as a function of temperature at $P = P_c$ using the Lennard-Jones potential with $r_c = 7.5\sigma$ and long range tail corrections. Full line: NIST values. Red line: ideal gas value. Dashed line: fitted function to MD results according to Eq. (10). (For interpretation of the references to colour in this figure legend, the reader is referred to the web version of this article.)

value to the ideal behavior along the critical isobar is patent. The fitted function reveals that it has a great agreement with NIST data especially for $\Delta T_r \leq 0.30$.

We also used MD to compute C_V at $\rho = 1.2\rho_c$ and C_P at $P = 1.2P_c$ to illustrate the applicability of the technique in thermodynamic paths distinct from those that exhibit the asymptotic behavior. It is expected that in these curves one can observe a maximum value of the thermodynamic property as a consequence of the proximity of the critical diverging path [30,65,66]. The MD results are shown in Fig. 6. By employing $r_c = 7.5\sigma$, the C_P values are in very good agreement with NIST data along all the curve. In contrast, C_V values fits well the NIST data for $\Delta T_r \geq 0.20$. The maximum value for C_P was found at $\Delta T_r = 0.05$ at $P = 1.2P_c$, whereas the maximum C_V at $\rho = 1.2\rho_c$ was not clearly distinguished. Results using other values for r_c are shown in Figs. S3 and S4 of the Supplementary material.

Fig. 3. Average reduced pressure as a function of temperature at $\rho = \rho_c$ obtained with NVT MD simulations to compute C_V of 10^4 argon atoms using the Lennard-Jones potential with $r_c = 7.5\sigma$ and long range tail corrections. Results are compared with NIST data.
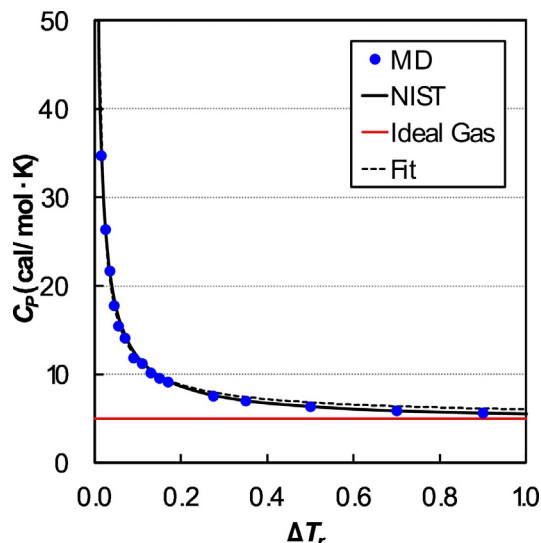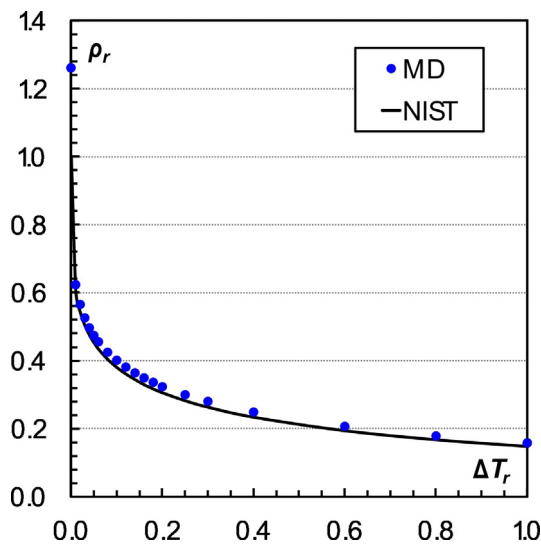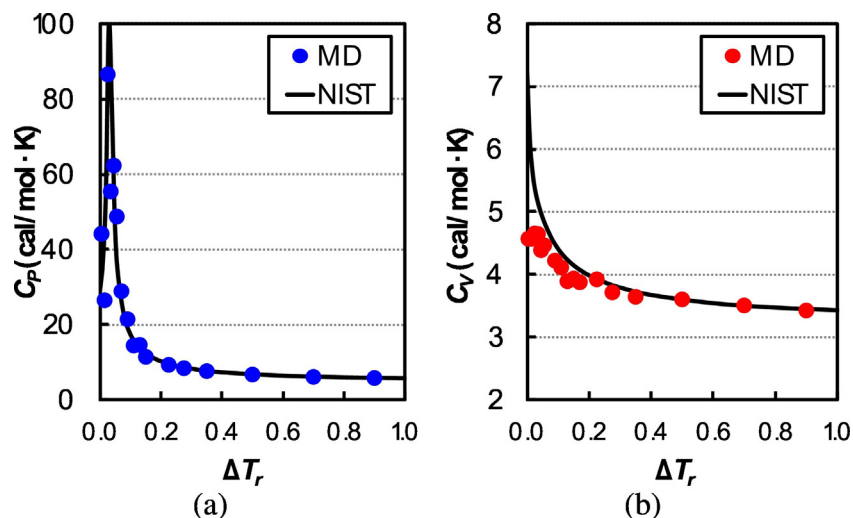

Fig. 5. Average reduced density as a function of ΔT_r at $P = P_c$ obtained with NPT MD simulations to compute C_P of 10^4 argon atoms using the Lennard-Jones potential with $r_c = 7.5\sigma$ and long range tail corrections. Results are compared with NIST data.

Fig. 6. Comparison between heat capacities obtained from NIST data and from MD simulations of 10^4 argon atoms as functions of temperature using the Lennard-Jones potential with $r_c = 7.5\sigma$ and long range tail corrections: (a) C_P at $P = 1.2P_c$ (b) C_V at $\rho = 1.2\rho_c$.

4. Conclusion

MD simulations were employed to compute heat capacities C_V and C_P of argon in the near-critical region. Good agreement of our results as compared with the NIST data was obtained in the whole range of reduced temperature ΔT_r. A careful use of the MD approach was indispensable to accurately describe the non-asymptotic critical divergences of C_V and C_P. In particular, the judicious choice of the cutoff radius combined with the use of long range tail corrections for the Lennard-Jones potential, and consequently the choice of the size of the simulation box, were shown to be crucial for the accuracy of the results.

We proposed an empirical model in the form of a power law that fairly describes the thermodynamic region where the critical effects are still observable but do not correspond to the asymptotic behavior. The critical effects on C_V and C_P continuously towards the ideal gas behavior could be described. For both properties, the computed exponents are different from those universal critical exponents.

Larger values of r_c were necessary to correctly describe critical divergences of C_V in comparison to NIST data. Whereas accurate results for C_P could be obtained with $r_c = 2.5\sigma$ and long range corrections, a value of 7.5σ was required for C_V. This is due to the lower amplitude of the anomalous behavior of C_V, which as compared to C_P, makes the former considerably more difficult to compute. The 10.0σ value did not improve the accuracy of results when compared to 7.5σ and considerably increased the computational time. We recommend the use of $r_c = 7.5\sigma$ for argon as the optimum value to be employed in MD simulations using a Lennard-Jones interaction potential to compute thermodynamics properties in the near-critical region.

We showed that the MD approach to compute near-critical properties is of general applicability. Investigations of other systems in the near-critical region using the same approach are underway. Furthermore, the presented procedure can be extended to smaller values of ΔT_r. For this purpose, it would be necessary to increase the size of the simulation box in order to refine the control of the temperature and to guarantee that the system size is larger than the correlation length. Naturally, there is a practical computational limit to this procedure. The universal critical exponents of the asymptotic power laws would be difficult to obtain with similar simulations since a temperature resolution below 10^{-5} is needed. In spite of that, the temperature resolution employed here was shown suitable to accurately describe the intermediate thermodynamic region between the asymptotic behavior and the mean field approach.

Appendix A. Supplementary data

Additional results of computed heat capacities C_V and C_P of argon are presented. Supplementary data associated with this article can be found in the online version, at 10.1016/j.molliq.2017.03.120.

References

[1] P. Carlès, J. Supercrit. Fluids 53 (2010) 2.
[2] M. Fisher, J. Math. Phys. 5 (1964) 944.
[3] D. Beysens, J. Straub, D. Turner, Phase transitions and near-critical phenomena, Fluid Sciences and Materials Science in Space, Springer-Verlag, Berlin 1987, pp. 221–256.
[4] J.V. Sengers, J.G. Shanks, J. Stat. Phys. 137 (2009) 857.
[5] N. Goldenfeld, Lectures on Phase Transition and the Renormalization Group, Perseus, 1992 Reading.
[6] P.C. Hohenberg, M. Barmatz, Phys. Rev. A 6 (1972) 289.
[7] I.B. Petsche, P.G. Debenedetti, J. Chem. Phys. 91 (1989) 7075.
[8] S.C. Tucker, M.W. Maddox, J. Phys. Chem. B 102 (1998) 2437.
[9] D.R. Biggerstaff, R.H. Wood, J. Phys. Chem. 92 (1988) 1988.
[10] E.H. Chimowitz, G. Afrane, Fluid Phase Equilib. 120 (1996) 167.
[11] National Institute of Standards and Technology, Thermophysical properties of fluid systems, Available: http://webbook.nist.gov/chemistry/fluid/ 2011.
[12] B. Widom, J. Chem. Phys. 43 (1965) 3898.
[13] K.G. Wilson, Phys. Rev. B 4 (1971) 3174.
[14] J.V. Sengers, J.M.H. Levelt Sengers, Annu. Rev. Phys. Chem. 37 (1986) 189.
[15] J.M.H. Levelt Sengers, J.V. Sengers, How close is "close to the critical point"? Perspectives in Statistical Physics 1981, pp. 239–272 (North-Holland, Amsterdam).
[16] J.A. White, J. Chem. Phys. 111 (1999) 9352.
[17] J.A. White, S. Zhang, Int. J. Thermophys. 19 (1998) 1019.
[18] J.A. White, S. Zhang, J. Chem. Phys. 99 (1993) 2012.
[19] H. Behnejad, J.V. Sengers, M.A. Anisimov, Thermodynamic behaviour of fluids near critical points, Applied Thermodynamics of Fluids, IUPAC, RSC, Cambridge 2010, pp. 321–367.
[20] D. Bolmatov, V.V. Brazhkin, K. Trachenko, Nat. Commun. 4 (2013) 2331.
[21] Z.Y. Chen, A. Abbaci, S. Tang, Phys. Rev. A 42 (1990) 4470.
[22] J. Nichele, L.S. de.B. Alves, I. Borges Jr., High Temp.-High Pressures 43 (2014) 385.
[23] J. Nichele, I. Borges Jr., A.B. de Oliveira, L.S. de B. Alves, J. Supercrit. Fluids 114 (2016) 46.

[24] H.B. Callen, Thermodynamics and a Introduction to Thermostatistics, second ed. John Wiley & Sons, New York, 1985.
[25] N.G. Polikhronidi, I.M. Abdulagatov, G.V. Stepanov, R.G. Batyrova, J. Supercrit. Fluids 43 (2007) 1.
[26] N.G. Polikhronidi, I.M. Abdulagatov, G.V. Stepanov, R.G. Batyrova, Fluid Phase Equilib. 252 (2007) 33.
[27] L.M. Radzhabova, G.V. Stepanov, I.M. Abdulagatov, Fluid Phase Equilib. 309 (2011) 128.
[28] S.M. Rasulov, L.M. Radzhabova, I.M. Abdulagatov, G.V. Stepanov, Fluid Phase Equilib. 337 (2013) 323.
[29] L.M. Radzhabova, G.V. Stepanov, I.M. Abdulagatov, K.A. Shakhbanov, Thermochim. Acta 575 (2014) 97.
[30] V.V. Brazhkin, Y.D. Fomin, A.G. Lyapin, V.N. Ryzhov, E.N. Tsiok, J. Phys. Chem. B 115 (2011) 14112.
[31] R. Haghbakhsh, M. Konttorp, S. Raeissi, C.J. Peters, J.P. O'Connell, J. Phys. Chem. B 49 (2014) 14397.
[32] T. Yigzawe, R. Sadus, J. Chem. Phys. 138 (2013) 194502.
[33] K. Binder, Mol. Phys. 108 (2010) 1797.
[34] A. Rizi, A. Abbaci, J. Mol. Liq. 171 (2012) 64.
[35] P. Ungerer, C. Nieto-Draghi, B. Rousseau, G. Ahunbay, V. Lachet, J. Mol. Liq. 134 (2007) 71.
[36] A. Davoodi, F. Feyzi, J. Mol. Liq. 150 (2009) 33.
[37] V.L. Kulinskii, N.P. Malomuzh, O.I. Matvejchukc, Phys. A 388 (2009) 4560.
[38] V.Yu. Bardik, N.P. Malomuzh, K.S. Shakun, V.M. Sysoev, J. Mol. Liq. 166 (2012) 1.
[39] N.P. Malomuzh, P.V. Makhlaichuk, S.V. Khrapatyi, Russ. J. Phys. Chem. A 88 (2014) 1450.
[40] H.E. Stanley, Introduction to Phase Transitions and Critical Phenomena, Oxford University Press, Oxford, 1971.
[41] G.O. Jones, P.A. Walker, Proc. Phys. R. Soc. B 69 (1956) 1348.
[42] A. Voronel, V.G. Gorbunova, V.A. Smirnov, N.G. Shmakov, V.V. Shchekochikhina, Sov. Phys. JETP 36 (1973) 505.
[43] A. Pelissetto, E. Vicari, Phys. Rep. 368 (2002) 549.
[44] M. Chandrasekhar, P.W. Schmidt, Phys. Rev. B 25 (1982) 6730.
[45] A. Rahman, Phys. Rev. A 136 (1964) 406.
[46] M.P. Allen, D.J. Tildesley, Computer Simulation of Liquids, Oxford University Press Oxford, 1987.
[47] D.C. Rapaport, The Art of Molecular Dynamics, Cambridge University Press, Cambridge, 2004.
[48] D. Frenkel, B. Smit, Understanding Molecular Simulation, second ed. Academic Press, San Diego, 2002.
[49] P.T. Cummings, Molecular simulation of near-critical and supercritical fluids, Supercritical Fluids: Fundamentals for Applications, Kluwer Academic Publishers Dordrecht 1994, pp. 387–409.
[50] S.J. Plimpton, J. Comput. Phys. 117 (1995) 1.
[51] H. Sun, J. Phys. Chem. B 102 (1998) 7338.
[52] G. Galliéro, C. Boned, A. Baylaucq, F. Montel, Phys. Rev. E 73 (2006) 061201.
[53] J.E. Jones, Proc. R. Soc. Lond. A 106 (1924) 463.
[54] A. Michels, H. Wijker, H.K. Wijker, Physica 15 (1949) 627.
[55] H. Okumura, F. Yonezawa, J. Chem. Phys. 113 (2000) 9162.
[56] J.J. Potoff, A.Z. Panagiotopoulos, J. Chem. Phys. 109 (1998) 10914.
[57] J. Pérez-Pellitero, P. Ungerer, G. Orkoulas, A.D. Mackie, J. Chem. Phys. 125 (2006), 054515. .
[58] H. Okumura, F. Yonezawa, J. Chem. Phys. 116 (2002) 7400.
[59] W. Shinoda, M. Shiga, M. Mikami, Phys. Rev. B 69 (2004) 134103.
[60] W. Shi, J.K. Johnson, Fluid Phase Equilib. 187-188 (2001) 171.
[61] F. Mandel, J. Chem. Phys. 59 (1973) 3907.
[62] A. Trokhymchuk, J. Alejandre, J. Chem. Phys. 111 (1999) 8510.
[63] J.K. Johnson, J.A. Zollweg, K.E. Gubbins, Mol. Phys. 78 (1993) 591.
[64] M.E. Fisher, Phys. Rev. A 136 (1964) 1599.
[65] L. Xu, P. Kumar, S.V. Buldyrev, S.H. Chen, P.H. Poole, F. Sciortino, H.E. Stanley, Proc. Natl. Acad. Sci. U. S. A. 118 (2005) 16558.
[66] G.G. Simeoni, T. Bryk, F.A. Gorelli, M. Krisch, G. Ruocco, M. Santoro, T. Scopigno, Nat. Phys. 6 (2010) 503.